OIKOS

Research article

Phytoplankton mean cell size and total biomass increase with nutrients are driven by both species composition and evolution of plasticity

Birte Matthiessen[1], **Giannina S. I. Hattich**[2,3], **Silvia Pulina**[4], **Thomas Hansen**[5], **Thorsten B. H. Reusch**[6] **and Jorin Hamer**[1]

[1]GEOMAR Helmholtz Centre for Ocean Research Kiel, Experimental Ecology, Kiel, Germany
[2]Åbo Akademi University, Environmental and Marine Biology, Åbo, Finland
[3]Department of Biology, University of Turku, Turku, Finland
[4]Aquatic Ecology Group, Department of Architecture, Design and Urban Planning, University of Sassari, Sassari, Italy
[5]GEOMAR Helmholtz Centre for Ocean Research Kiel, Central Lab for Chemical Analytics, Kiel, Germany
[6]GEOMAR Helmholtz Centre for Ocean Research Kiel, Marine Evolutionary Ecology, Kiel, Germany

Correspondence: Birte Matthiessen (bmatthiessen@geomar.de)

Oikos
2024: e10910
doi: 10.1111/oik.10910

Subject Editor: Silke Langenheder
Editor-in-Chief: Dries Bonte
Accepted 22 September 2024

Community trait variability can arise from the species, genotypic, or individual plastic level. Trait changes on these levels can occur simultaneously, interact, and potentially translate to community functioning. Thus, they are crucial to realistically predict community functional changes. Using a phytoplankton model community comprising a diatom and a coccolithophore each with nine genotypes varying in cell size, we conducted a selection experiment over 130 generations towards nutrient availability. According to our expectations, mean community cell size and total biomass increased with increasing nutrient availability. Interspecifically, these community level changes were driven by shifts in species composition towards the larger diatom. Changes caused by intraspecific shifts did not result from sorting according to genotypes' standing variation in cell size in the first place. Instead, intraspecific changes likely resulted from the selection for a highly plastic diatom genotype, which led to a phenotypic distribution with larger cells in high and smaller cells in lower nutrient concentrations. We suggest that besides interspecific species sorting, the evolution of size plasticity through genotype selection represented an intraspecific contribution to mean community size increase with increasing nutrient availability that ultimately translated to increased total biomass. Our results demonstrate that all three levels on which trait changes can occur, regulate phytoplankton community-level functional changes and thus should be considered when predicting community change on ecological time scales.

Keywords: Chaetoceros affinis, community functioning, Emiliania huxleyi, plasticity, species and genotype sorting, trait diversity

NORDIC SOCIETY OIKOS

www.oikosjournal.org

Introduction

Mean trait and functional changes in biological communities are due to diversity shifts that are driven by different underlying processes involving ecological, evolutionary, and physiological dynamics and occur among and within species. Interspecific trait changes are driven by species compositional shifts and intraspecific changes by evolutionary dynamics and phenotypic plasticity. Trait variability on the different organisational levels can be of similar magnitude (Schaum et al. 2013, Siefert et al. 2015) and changes, e.g. evolutionary changes and species turnover, can occur on similar time scales (Hairston Jr et al. 2005, Fussmann et al. 2007, Govaert et al. 2016, Des Roches et al. 2018, Raffard et al. 2019). Therefore, both inter- and intraspecific trait diversity shifts are potentially important for community-level changes (Govaert et al. 2016, Des Roches et al. 2018, Raffard et al. 2019).

The consequences of species diversity for ecosystem functioning and services, mediated by community mean trait changes, have been comprehensively demonstrated (reviewed by Cardinale et al. 2012). Species diversity effects were explained by niche partitioning among the species that form a community and sequester the available resources into biomass (i.e. realised productivity) as one important measure of ecosystem functioning (Cardinale et al. 2007, 2009, Gross and Cardinale 2007). The potential role of intraspecific diversity for community functioning gained attention only recently. Similarly shaped saturated relationships between diversity and ecosystem functioning have been shown for both species (reviewed by Cardinale et al. 2012) and intraspecific (Raffard et al. 2019) diversity. Moreover, intraspecific diversity can affect ecological dynamics with a similar effect size to species diversity (Raffard et al. 2019). This can likely be related to the fact that intraspecific trait variability can be of similar magnitude as interspecific variability as shown by a global meta-analysis covering 36 functional traits in several hundreds of plant communities (Siefert et al. 2015). Particularly the role of evolutionary changes due to genotype sorting from standing genetic variability was suggested to alter community-level changes (Ellers 2009, Litchman et al. 2012, Lohbeck et al. 2012, Listmann et al. 2020) but so far has rarely been demonstrated to affect community functioning via shifts in community-level trait values (Hattich et al. 2023). Additionally, the ecophysiology of individual genotypes, i.e. their phenotypic plasticity as another component of intraspecific variability, can be significant (Jacob and Legrand 2021, Valladares et al. 2000). Its potential role in affecting community mean trait values and functioning, however, is still subject to investigation. For example, Hattich et al. (2017) demonstrated that in order to measure a realistic mean response variability to environmental change of a phytoplankton species, it is necessary to take both the phenotypic plasticity of particular genotypes and the variability among them into account. It was shown that predictions on community assembly and coexistence can change significantly when considering intraspecific trait variability instead of using fixed species mean trait values (Violle et al. 2012), which in turn can have significant consequences for community functioning. Furthermore, interactions among simultaneously changing trait diversity on the different levels of biological organisation can be important. Eco-evolutionary dynamics are a prominent example of such interactions that were shown to translate to altered community dynamics (Fussmann et al. 2007, Koch et al. 2014). Another example is the evolution of plasticity in multiple morphological, life history, and behavioural traits of *Daphnia magna* in response to changes in fish predation (Stoks et al. 2016). Taken together, these aspects point to the necessity to better understand the simultaneous and potentially interacting underlying inter- and intraspecific dynamics that drive community-level trait changes and importantly their functional consequences in response to changing environmental conditions.

Understanding the causes and predicting the functional consequences of community change by using phytoplankton as a model system has been a cornerstone in community ecology (Hutchinson 1961, Sommer 1984, Sommer and Worm 2002). Due to their vast population sizes and fast generation times, and their well-understood community ecology, phytoplankton lend themselves as an ideal model system to add another layer of complexity to study the community-level consequences of simultaneous inter- and intraspecifically driven trait changes. One major recent advance was to use trait-based approaches to simplify the taxonomic complexity and by that to identify important tradeoffs among phytoplankton traits that ultimately explain community changes (Litchman 2007, Litchman and Klausmeier 2008, Litchman et al. 2015). In particular, traits affecting the acquisition and utilisation of primary resources such as nutrients and light, along with traits modulating losses due to grazing and sinking were useful in this respect. Cell size is an important 'master' trait that directly or indirectly influences these four aspects that make up the phytoplankton ecological niches (reviewed by Maranon 2015, Sommer et al. 2016, Hillebrand et al. 2022) and as such can help to predict the configuration and functioning of plankton communities (Sommer et al. 2002, Lewandowska et al. 2014, Acevedo-Trejos et al. 2018, Paul et al. 2021). Major phytoplankton groups span up to 4 orders of magnitude in linear cell dimension (Finkel et al. 2010). Small phytoplankton show higher affinity for nutrients and lower diffusion limitation due to their higher surface-to-volume ratios (Aksnes and Egge 1991, Hein et al. 1995, Edwards et al. 2012). Thus, in nutrient-limited conditions small cells are competitively superior over larger cells and nutrient-poor regions or seasons are dominated by small phytoplankton, for example by picoplankton, small flagellates, or coccolithophores (Lewandowska et al. 2014, Litchman et al. 2015). Larger cells, for example diatoms, are better competitors in nutrient replete and/or pulsed conditions because they are characterised by high uptake and growth rates and/or storage capacities while showing lower affinity for nutrients (Sommer 1984, Edwards et al. 2012, Maranon 2015, Sommer et al. 2016). Cell size in phytoplankton, however, does not only vary interspecifically but also among and within clonal cultures of species and was

shown to affect nutrient uptake and utilisation-related traits (Malerba et al. 2016). In fact, it has been shown for a natural phytoplankton community that cell size changes in response to sea surface warming occur both inter- and intraspecifically (Peter and Sommer 2012, 2013). Their role for community-level size shifts, however, remained unexplained.

To understand community-level trait shifts that are potentially driven by simultaneous inter- and intraspecific diversity changes in phytoplankton, we conducted two experiments: one long-term community experiment and one short-term plasticity experiment, both treated with different nutrient regimes. The two species in the model community, a diatom and a coccolithophore, and their genotypes significantly differed in cell size, with the diatom genotypes showing greater variability. Considering that size variability was present between and within the species, we expected both inter- and intraspecific selection on this standing trait diversity in the long-term experiment. According to the relationship between cell size and competitive ability in different nutrient regimes, we expected that low nutrient concentrations select for the smaller species and genotypes and vice versa that higher nutrient concentrations select for larger species and genotypes. We assumed the degree of intraspecific cell size changes due to phenotypic plasticity for the diatom to be minor because it should be limited to the alteration in the diatom's cell height (i.e. the pervalvar axis of the cylindric cell) during asexual cell growth, while the diameter (i.e. the girdle band length) can only be altered through auxosporulation which usually involves sexual reproduction (Kaczmarska et al. 2013). Therefore, we expected that a change in mean cell size, total abundance and biomass can be mainly explained by both species and genotype diversity shifts.

Material and methods

Model system and general experimental set-ups

The model system consisted of two phytoplankton species, the diatom *Chaetoceros affinis* and the coccolithophore *Emiliania huxleyi*, comprising nine genotypes each. The genotypes were originally collected and isolated from coastal waters off Gran Canaria, Spain, in 2014 and 2015 (27°59′N, 15°22′W). For detailed information on genotypes and dates of collection, see Hattich et al. (2017).

Both the community and the plasticity experiment were conducted in 0.5 litre polycarbonate bottles filled with 540 ml sterile filtered (0.2 µm) artificial seawater with full marine salinity of 35 prepared after (Kester et al. 1967). Whereas micronutrients, vitamins and trace metals were added according to f/8 concentration (Guillard 1975) in both experiments, the addition of macronutrients varied because of the experimental nutrient treatments. To prevent phytoplankton sedimentation, the bottles were fixated on a plankton wheel that constantly rotated at a speed of 0.75 min^{-1}. The plankton wheel with bottles was located in a temperature-controlled (21.9 ± 0.6°C) climate chamber underneath an LED light facility that provided the phytoplankton with a 17:7 light/dark cycle (3 h sunrise and sunset) and a maximum light intensity of 300 ± 21.0 µmol photons m^{-2} s^{-1}.

Community experiment

In order to simultaneously follow species and genotype diversity shifts that potentially explain community mean trait and functional changes, we conducted a long-term community experiment. The two species grew in semi-continuous batch cycles of seven days each, which allowed for stable coexistence. Over each weekly culture cycle, the initially replete nutrients were favourable to the diatom, while the coccolithophore gained when nutrients were low at the end (Hamer et al. 2022). Standing genotype variability in both species was introduced by initiating the experiment with the nine genotypes each. The model community was treated with three different nutrient regimes. While ortho-phosphate was added in constant concentrations of 0.9 ± 0.1 µmol l^{-1}, nitrate was manipulated in three different concentrations of 9.0 ± 0.7, 19.6 ± 0.8, or 29.9 ± 0.9 µmol l^{-1} and thus reflected N:P ratios of approximately 10, 20 and 30, respectively. We hereafter refer to the three nutrient regimes as 10, 20 and 30 N. Silicate was added in concentrations to reflect a 4:1 N:Si ratio. The three different growth media (i.e. nutrient regimes) were prepared prior to filling the experimental bottles. Each of the three nutrient regimes was five-fold replicated.

Prior to the experimental start, genotypes were separately acclimated to experimental conditions with 20 µmol l^{-1} nitrate for seven days. Mean cell size of 15 cells of each genotype during acclimation was measured as described below. To compensate for the species' significant different cell sizes both species were initially inoculated in equal biovolumes, which equalled 25 cells ml^{-1} for *C. affinis* and 500 cells ml^{-1} for *E. huxleyi*. The nine genotypes of each species initially contributed with equal cell abundances. The experimental duration was 182 days which summed up to 26 batch cycles and corresponded to approximately 130 phytoplankton generations.

To weekly measure community composition and species' and community biomass, abundance and mean cell size, the experimental bottles were sampled under a clean bench at the end of each batch cycle (NuAire, model: NU-480-400E). At the same time, a defined proportion (biovolume of 2.88×10^7 ± 1.57×10^7 μm^3) of the community was transferred to the next batch cycle with fresh medium. To measure the abundance of *E. huxleyi*, 3 ml were sampled over a sieve with 20 µm mesh size, separating the small *E. huxleyi* from the larger *C. affinis* cells. Subsequently, the separated *E. huxleyi* cells were counted with a flow cytometer (Gallios, Beckmann Coulter). To determine the abundance of *C. affinis*, 5 ml samples were fixed with Lugol's iodine solution and counted using an inverted light microscope. Cell size measurements of both species were likewise conducted microscopically after Hillebrand et al. (1999). Originally, the cell size of five randomly picked cells of each species was measured at the end of batch cycles 1, 2, 3, 6, 7, 8, 9, 10, 11, 12, 13, 17, 22, 23 and 26. Due to observed high size variability of *C. affinis* cells, the protocol was adjusted for

the at that time not yet measured batch cycles to reach a higher precision in size measurements. In the adjusted protocol *C. affinis* cells were classified into three morphotypes based on their diameter (girdle band length; small: < 6 µm, medium: 6–12 µm, large: > 12 µm) from which five randomly picked cells were measured at the end of batch cycles 4, 5, 14, 15, 16, 18, 19, 20, 21, 24 and 25. In the adjusted protocol the morphotype's abundances were counted separately which allowed us to quantify the morphotype's distribution and calculate mean cell size standardised to their distribution. Biovolume per ml was calculated from the size and abundance measurements and used as a proxy for biomass. Evenness was expressed as the relative contribution of *E. huxleyi* biomass to total biomass. Temporal dynamics of response variables' variability in the system were shown as coefficients of variation (CV). At the end of batch cycle 1, 7, 13 and 26 samples were taken for analyses of dissolved inorganic nutrients.

To analyse genotype composition over time, samples were taken after 7, 13 and 26 batch cycles. From each experimental bottle ten cells of *E. huxleyi* and *C. affinis*, respectively, were re-isolated for assessment of genotype composition using microsatellite fragment analysis (for detailed information see the Supporting information). Allele binning was performed using GeneMarker software and identification of multi-locus genotypes was done by comparing the primer peaks of the reisolates with the primer peaks of the original genotypes. For analysis of genotype sorting over time, experimental units with less than five isolates of one species identified were excluded. To link the remaining *C. affinis* genotypes at the end of the experiment (batch cycle 26) to their emerging plasticity and morphotype distribution, we also included experimental units with less than five isolates. The reason was, that at this time point only one genotype was found per experimental unit in all cases, to which we hereafter refer to as monodominance.

Plasticity experiment

In order to test, whether the observed size variability of *C. affinis* genotypes at the end of the community experiment was due to selection from standing short-term genotype size plasticity or not, we determined the size reaction norm of each *C. affinis* genotype over a gradient of seven nitrate concentrations (Table 1) over one batch cycle (n = 3). Prior to the plasticity experiment, each genotype was acclimated over two weeks at initial nutrient concentrations of 1.8 µmol l^{-1} P, 30 µmol l^{-1} N and 40 µmol l^{-1} Si. Nutrient concentrations in both experiments were measured with an autoanalyzer (Seal Analytical QuAAtro). At the end of the experiment the size of five randomly picked cells of each morphotype (diameter: small: <5 µm, medium: 5–10 µm, large: >10 µm) present in each bottle were measured microscopically as explained above. From these measurements, standardised to the morphotype's distribution, the mean cell size of each genotype was determined. For unknown reasons *C. affinis* genotype B68 showed much lower cell numbers in the 20 N, 30 N and 40 N nutrient regimes in comparison to the other *C. affinis* genotypes, while nitrate (4.6–16 µmol l^{-1}), silicate (15.4–21.4 µmol l^{-1}), and phosphate (0.5–0.9 µmol l^{-1}) were still present, suggesting that stationary phase has not been reached. In consequence, we excluded this genotype from further comparative analyses.

In both experiments cell size variability was expressed as each genotype's size range of mean values measured at the different nutrient levels. Among genotype variability in the plasticity experiment was expressed as the size range of mean sizes of each genotype across nutrient levels.

Statistical analyses

Total biomass (measured as biovolume ml^{-1}) and cell abundance, *C. affinis* biomass and cell size, *E. huxleyi* biomass and cell size, evenness, and mean community cell size were analysed using generalized additive mixed-effects models (GAMM) with the categorical factor Nutrient regime, the smooth term Time, and their interaction. Bottle identity was incorporated as a random factor to account for repeated measures. Coefficients of variation for total biomass, mean cell size of the community and of *C. affinis* and *E. huxleyi* were analysed using linear mixed-effects models (LMM) with the fixed effect Time and the random effect Nutrient regime. Cell sizes of the two species prior to the community experiment were compared using Welch's t-test and those of the genotypes by using analyses of variance (ANOVA) for each species.

The assumptions for robust model testing were validated graphically, and the significance level α for all analyses was set to 5%. All statistical analyses were done using R software and additional packages 'lme4' (Bates et al. 2015), 'lmerTest' (Kuznetsova et al. 2017), 'mgcv' (Wood 2011), and 'itsadug' (van Rij et al. 2022).

Table 1. Nominal and actual starting nutrient concentrations and resulting N:P ratios at the onset of the plasticity experiment with *C. affinis*.

Nitrate (µmol l^{-1})		Phosphate (µmol l^{-1})		Silicate (µmol l^{-1})		N:P	
nominal	actual	nominal	actual	nominal	actual	nominal	actual
2.5	2.4	2	1.9	3.75	2.9	1.25	1.30
5	4.8	2	1.9	7.5	7.1	2.5	2.56
7.5	7.3	2	1.9	11.25	10.9	3.75	3.86
12.5	12.1	2	1.9	18.75	18.0	6.75	6.51
20	19.5	2	1.9	30	29.0	10	10.40
30	29.2	2	1.9	45	43.7	15	15.48
40	38.6	2	1.9	60	47.7	20	20.60

Results

Community and species-level responses of biomass, composition, abundance and cell size

Both species coexisted in all nutrient regimes throughout the experiment. Total biomass significantly increased with nitrate availability (Fig. 1, Table 2). In particular, comparing the 10 to 20 N treatment, total biomass increased on average by 122%, driven by increases in the absolute biomass of both species (Fig. 1, Table 2). The even biomass distribution between the two species thus did change only marginally from the 10 to 20 N nutrient regime (Fig. 1, Table 2). With further increasing nitrate concentration, *C. affinis* became dominant and evenness sharply declined as a consequence (Fig. 1, Table 2). Total cell abundance was highest in the 10 and 20 N due to the relatively high contribution of the smaller *E. huxleyi* cells and more than halved in the 30 N nutrient regime (Fig. 1, Table 2).

Mean community cell size significantly increased with nitrate concentration and showed the largest cells in the 30 N nutrient regime (Fig. 1, Table 2). Specifically, mean cell size increased on average by 60% (136–216 μm^3) from the 10 to 20 N and by another 372% (216–1021 μm^3) from the 20 to 30 N nutrient regime. Intraspecifically, cell size of both species increased in response to nutrients. *Emiliania huxleyi* cell size increased by on average 20% from one increasing N regime to the other (10 N: 43 μm^3; 20 N: 51 μm^3; 30 N: 61 μm^3; Fig. 2, Table 2). Cell size of *C. affinis* increased by 20% (995–1207 μm^3) comparing the 10 N to the 20 N nutrient regime, and by an additional 30% (1207–1569 μm^3) comparing the 20 and 30 N treatments. (Fig. 2, Table 2).

Towards the end of the long-term experiment, mean community and *C. affinis* cell size more than doubled from day 120 onwards in the 20 and 30 N treatments. At the same time, in the 30 N and to a lesser degree also in the 20 N treatment, total and *C. affinis* biomass and dominance further increased, while total abundance declined with time (Fig. 1, 2, Table 2, Supporting information). Variability of mean community and *C. affinis* cell size and total biomass increased with time in all treatments, whereas *E. huxleyi* cell size variability was not affected (Fig. 1, 2, Supporting information).

Genotype composition

The temporal dynamics of genotype composition in response to nutrient regimes showed a clear direction towards genotype competitive exclusion. Whereas for *E. huxleyi* from approximately 100 days onwards the same genotype (C91) dominated in all treatments (Fig. 3A), for *C. affinis* three different genotypes (B13, B67, B82) remained present in the different nutrient regimes until the end of the experiment (Fig. 3B). These genotypes, however, never co-occurred in one bottle, regardless of whether experimental units with less than five isolates of one species identified were excluded or not (Fig. 3B, Supporting information). Instead, they exclusively dominated different replicates of the same nutrient treatment, i.e. were monodominant. In more detail, from approximately 100 days onwards *C. affinis* genotype B67 was most abundant. It monodominated all replicates in the 20 N but also individual replicates of the 10 N and 30 N nutrient regimes. Genotype B82 monodominated one replicate of the 10 N and one of the 30 N nutrient regimes and B13 monodominated only one replicate of the 30 N nutrient regime. The monodominance of genotypes at the end of the

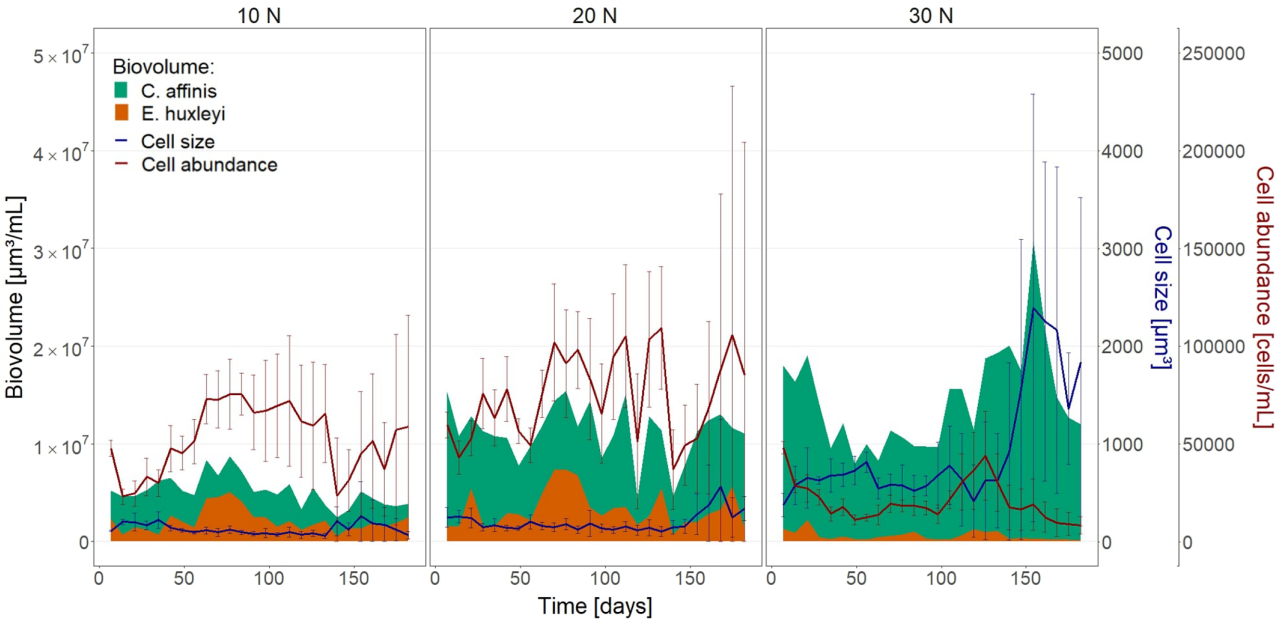

Figure 1. Species contributions (*E. huxleyi* in orange and *C. affinis* in green) (as mean total biovolume ± SD), total cell abundance and mean community cell size in the three different nutrient regimes 10, 20 and 30 µmol l^{-1} N.

Table 2. Outcome of generalized additive mixed-effects models (GAMM) testing the effects of the categorical factor Nutrient regime, the smooth term Time, and their interaction on the response variables total biomass, total cell abundance, mean cell size, evenness, *C. affinis* biovolume and cell size, *E. huxleyi* biovolume and cell size. Significance levels for p-value: 0 '***' 0.001 '**' 0.01 '*' 0.05 '.' 0.1 ' ' 1.

Total biomass, n = 373 Expl deviance = 66.7%	Estimate	Standard error	t-value	p-value
Intercept	7.01405	0.01750	400.86	$< 2 \times 10^{-16}$ ***
10 N	−0.33451	0.02475	−13.52	$< 2 \times 10^{-16}$ ***
30 N	0.09130	0.02495	3.66	0.000292 ***
Smooth terms	**Estimated df**	**Reference df**	**F-value**	**p-value**
s(Time)	16.775	20.158	3.998	$< 2 \times 10^{-16}$ ***
s(Time:20 N)	1.001	1.001	1.976	0.1608
s(Time:10 N)	2.613	3.249	3.117	0.0262 *
s(Time:30 N)	3.859	4.927	7.573	1.95×10^{-6} ***
s(Bottle ID)	3.722	12.000	0.447	0.1448
***E. huxleyi* biomass**, n = 375 Expl deviance = 75.9%.	**Estimate**	**Standard error**	**t-value**	**p-value**
Intercept	6.39323	0.07604	84.077	$< 2 \times 10^{-16}$ ***
10 N	−0.20006	0.10751	−1.861	0.0637.
30 N	−0.83774	0.10766	−7.781	9.11×10^{-14} ***
Smooth terms	**Estimated df**	**Reference df**	**F-value**	**p-value**
s(Time)	20.60	23.41	8.767	$<2 \times 10^{-16}$ ***
s(Time:20 N)	1.000	1.000	0.108	0.743
s(Time:10 N)	4.588×10^{-5}	9.159×10^{-5}	0.014	0.999
s(Time:30 N)	6.661	7.778	11.897	$<2 \times 10^{-16}$***
s(Bottle ID)	10.70	12.00	8.013	$<2 \times 10^{-16}$***
***C. affinis* biomass,** n = 381 Expl. deviance = 61.4%	**Estimate**	**Standard error**	**t-value**	**p-value**
Intercept	6.82217	0.03565	191.383	$< 2 \times 10^{-16}$***
10 N	−0.40549	0.05041	−8.043	1.25×10^{-14}***
30 N	0.25566	0.05041	5.071	6.31×10^{-07}***
Smooth terms	**Estimated df**	**Reference df**	**F-value**	**p-value**
s(Time)	1.0001	1.0002	6.166	0.013472 *
s(Time:20 N)	0.1005	0.1939	0.037	0.932648
s(Time:10 N)	2.3491	2.9256	2.350	0.064295 .
s(Time:30 N)	3.9674	4.8981	5.424	0.000112 ***
s(Bottle ID)	7.6051	12.0000	1.726	0.001480 **
Evenness, n = 373 Expl. deviance: 71.5%	**Estimate**	**Standard error**	**t-value**	**p-value**
Intercept	5.2153	0.3053	17.080	$< 2 \times 10^{-16}$ ***
10 N	0.8199	0.4318	1.899	0.0585 .
30 N	−3.2589	0.4327	−7.532	4.44×10^{-13}***
Smooth terms	**Estimated df**	**Reference df**	**F-value**	**p-value**
s(Time)	7.766	9.455	6.065	$< 2 \times 10^{-16}$ ***
s(Time:20 N)	1.002	1.003	3.039	0.08190 .
s(Time:10 N)	4.378	5.355	2.833	0.01746 *
s(Time:30 N)	2.911	3.815	4.580	0.00246 **
s(Bottle ID)	10.209	12.000	5.790	$< 2 \times 10^{-16}$ ***
Tot abundance, n = 385 Expl. deviance: 76.7%	**Estimate**	**Standard error**	**t-value**	**p-value**
Intercept	4.79888	0.05458	87.929	$< 2 \times 10^{-16}$ ***
10 N	−0.15440	0.07718	−2.000	0.0462 *
30 N	−0.55357	0.07717	−7.173	4.45×10^{-12} ***
Smooth terms	**Estimated df**	**Reference df**	**F-value**	**p-value**
s(Time)	13.837	16.102	5.312	$<2 \times 10^{-16}$***
s(Time:20 N)	1.000	1.000	5.652	0.0180 *
s(Time:10 N)	3.663	4.525	2.697	0.0218 *
s(Time:30 N)	5.502	6.623	10.700	$<2 \times 10^{-16}$ ***
s(Bottle ID)	11.001	12.000	11.018	$<2 \times 10^{-16}$ ***
Mean comm cell size, n = 373 Expl. deviance: 78%.	**Estimate**	**Standard error**	**t-value**	**p-value**
Intercept	2.21134	0.05441	40.643	$< 2 \times 10^{-16}$ ***
10 N	−0.17957	0.07695	−2.334	0.0202 *
30 N	0.63774	0.07707	8.275	2.84×10^{-15} ***

(Continued)

Table 2. Continued.

Total biomass, n = 373 Expl deviance = 66.7%	Estimate	Standard error	t-value	p-value
Smooth terms	**Estimated df**	**Reference df**	**F-value**	**p-value**
s(Time)	6.452	7.481	3.335	0.00133 **
s(Time:20 N)	2.767	3.325	1.759	0.24596
s(Time:10 N)	3.501	4.254	2.794	0.02752 *
s(Time:30 N)	1.856	2.443	0.542	0.58688
s(Bottle ID)	10.523	12.000	7.066	$< 2 \times 10^{-16}$ ***
***E. huxleyi* cell size**, n = 375 Expl. deviance: 51.9%.	**Estimate**	**Standard error**	**t-value**	**p-value**
Intercept	1.65278	0.01782	92.748	$<2 \times 10^{-16}$ ***
10 N	−0.06499	0.02517	−2.582	0.0102 *
30 N	0.06373	0.02536	2.513	0.0124 *
Smooth terms	**Estimated df**	**Reference df**	**F-value**	**p-value**
s(Time)	20.84	23.57	11.732	$<2 \times 10^{-16}$ ***
s(Time:20 N)	1.686	2.086	0.606	0.532
s(Time:10 N)	1.744	2.161	2.170	0.127
s(Time:30 N)	1.411×10^{-4}	2.394×10^{-4}	0.160	0.995
s(Bottle ID)	4.104	12.00	0.521	0.113
***C. affinis* cell size**, n = 381 Expl. deviance: 49.6%				
Intercept	3.01580	0.03729	80.864	$<2 \times 10^{-16}$ ***
10 N	−0.07048	0.05274	−1.336	0.1823
30 N	0.09827	0.05274	1.863	0.0633 .
Smooth terms	**Estimated df**	**Reference df**	**F-value**	**p-value**
s(Time)	1.000	1.000	1.796	0.1811
s(Time:20 N)	5.387	6.520	10.700	$<2 \times 10^{-16}$ ***
s(Time:10 N)	3.022	3.962	2.397	0.0427 *
s(Time:30 N)	3.854	4.763	11.555	$<2 \times 10^{-16}$ ***
s(Bottle ID)	9.674	12.000	4.145	$<2 \times 10^{-16}$ ***

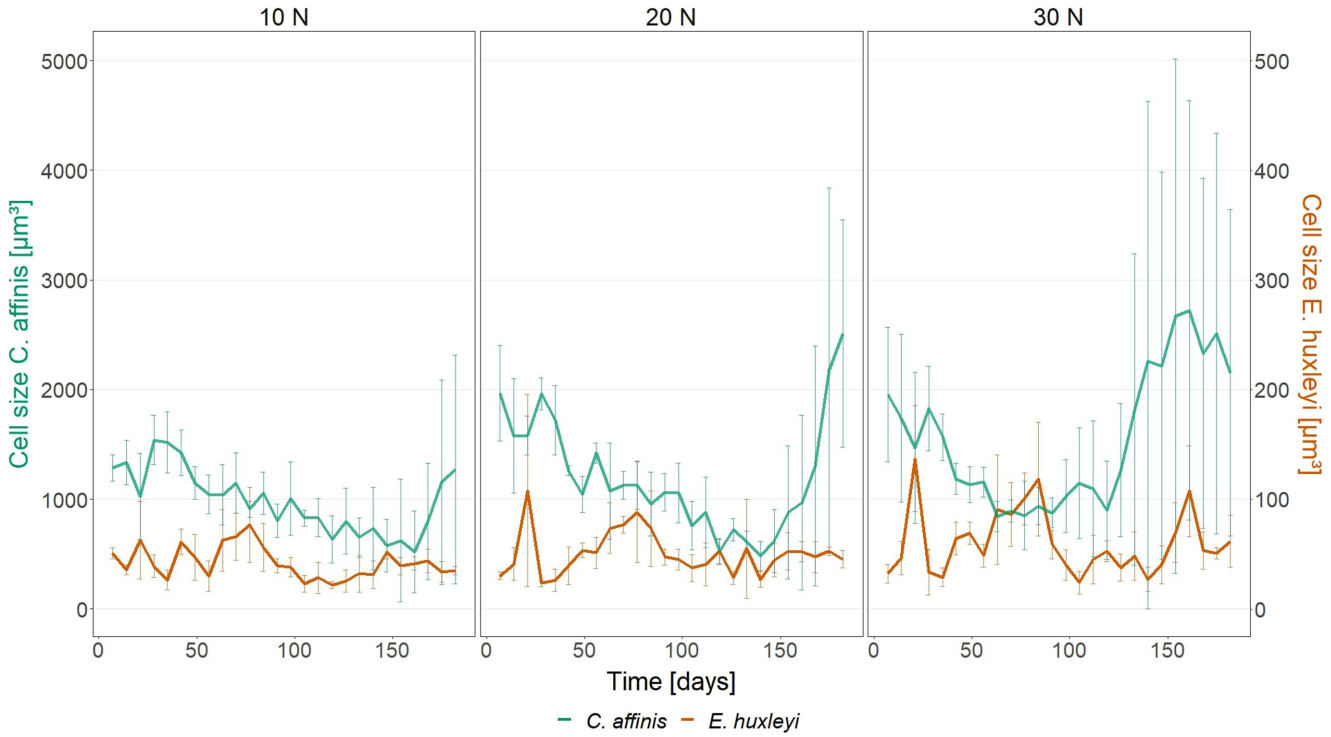

Figure 2. Mean cell size (± SD) of *E. huxleyi* (orange line) and *C. affinis* (green line) in response to nutrient regimes.

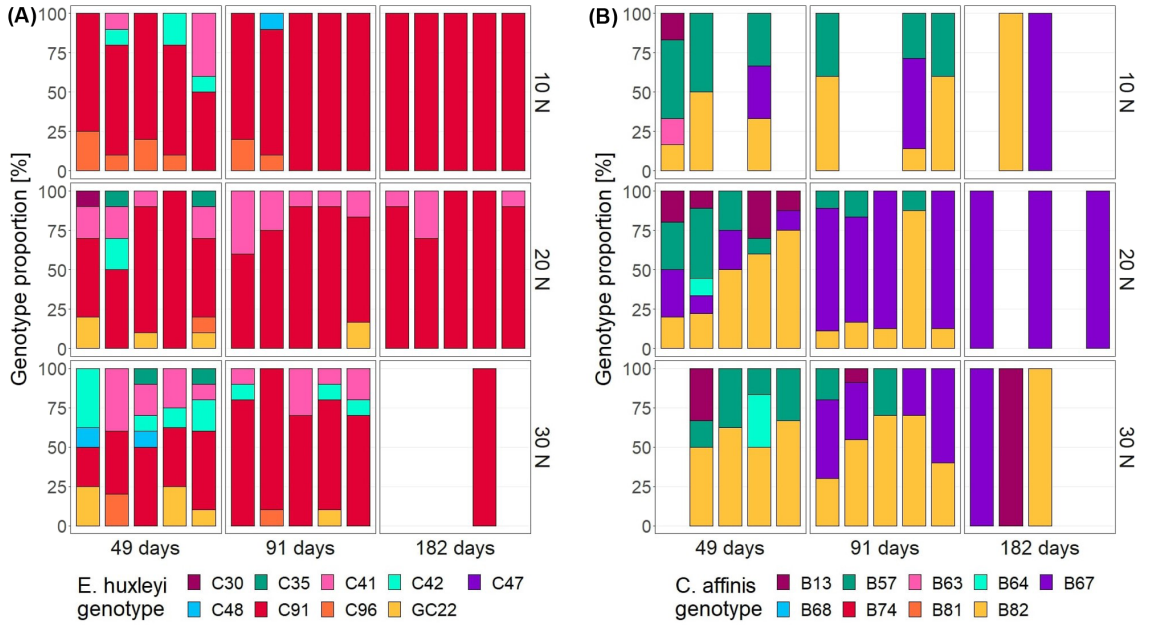

Figure 3. Temporal dynamics of the relative abundances of (A) *E. huxleyi* and (B) *C. affinis* genotypes in response to nutrient regimes. Experimental units for each nutrient regime at the different time points are displayed next to each other. Experimental units with less than five identified isolates were excluded.

experiment allowed us to measure the remaining genotype's cell size variability in response to nutrients.

Initial cell size

Prior to the long-term community experiment, the two species differed in cell size with *E. huxleyi* genotypes being significantly smaller (135 ± 43 µm³ SD) than *C. affinis* (1361 ± 868 µm³ SD; Supporting information; Welch's t-test: $t = 15.448$, $df = 119.52$, p-value $< 2.2 \times 10^{-16}$). While genotype identity of *E. huxleyi* explained only 23% of the total variation in the species' size ($\eta^2 = 0.23$, Supporting information; ANOVA: $F_{8,126} = [4.6246]$, $p = 5.693 \times 10^{-05}$), mean cell size of *C. affinis* genotypes differed markedly ($\eta^2 = 0.86$; Supporting information; ANOVA: $F_{7,112} = [98.879]$, p-value $\leq 2.2 \times 10^{-16}$). Here, genotype identity explained 86% of the variation in the species' size. *C. affinis* genotypes formed two size clusters of four small (B63, B67, B74, B81) and four larger genotypes (B13, B57, B64, B82), respectively, spanning a range of 1480 µm³ between the small (620 µm³) and the large (2100 µm³) genotypes (Supporting information).

Observed cell size variability, distribution of morphotypes, and short-term reaction norms of *C. affinis*

The three remaining *C. affinis* genotypes at the end of the community experiment (B13, B67, B82) exhibited variation in mean cell size after approximately 130 generations of nutrient selection that ranged from on average 955 to 4223 µm³ across nutrient treatments (Fig. 4). This significant variation in cell size was driven by the most abundant (B67) among the remaining monodominant genotypes (Fig. 3B). The phenotypic size variation of genotype B67 ranged from on average 1501 and 2888 µm³ in the 10 and 20 N treatments, respectively, up to 4223 µm³ in the 30 N nutrient regime (means with standard deviations in Fig. 4), spanning a size range of 2722 µm³. In fact, the cell size range of genotype B67 across nutrient regimes at the end of the long-term community experiment exceeded the genotype's short-term reaction norm in cell size by almost 7-fold (673%) (compare short-term plasticity vs. observed long-term variability in cell size of B67 in Fig. 5), and that of all other *C. affinis* genotypes by on average 522% (compare short-term plasticity of all genotypes except for B67 with observed long-term variability in cell size of B67 in Fig. 5). The exceedance of the observed size variability in the long-term experiment compared to short-term size plasticity is noteworthy, because long-term responses were measured over a smaller nutrient gradient (9–30 µmol nitrate l^{-1}) compared to the gradient applied in the short-term plasticity experiment (2.5–40 µmol nitrate l^{-1}).

The unexpectedly high variability in mean cell size across the three nutrient regimes, particularly exhibited by genotype B67, resulted from the underlying morphotypes' distribution (Fig. 4). For genotype B67 only the large morphotype contributed to the genotype's absolute biomass in the 30 N nutrient regime. In the 10 and 20 N nutrient regimes, besides the large, the small and the medium size classes contributed, respectively. For *C. affinis* genotype B82 that remained in individual replicates of the 10 and 30 N nutrient regimes, only the medium-sized morphotype contributed to its absolute biomass in the 30 N and both the large and small morphotypes contributed in the 10 N nutrient regime. Average cell size due to this morphotype distribution equalled out to

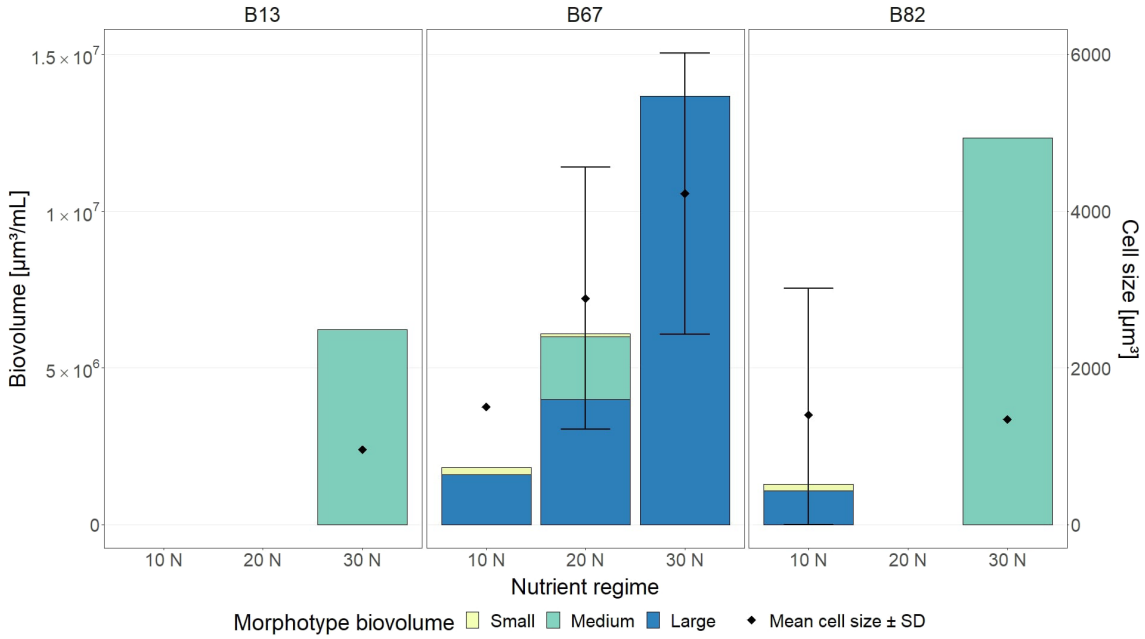

Figure 4. Biomass of the three *C. affinis* genotypes (B13, B67, B82) persisting in the different nutrient regimes until the end of the long-term community experiment (175 days). The colours indicate the contributions of morphotypes to the absolute genotype's biomass and the point and whisker plots the resulting mean cell size (± SD) of the genotype.

cells of on average 1370 µm³ in both nutrient regimes. Only the medium sized morphotype contributed to the absolute biomass of *C. affinis* genotype B13 that remained to the end of the community experiment in only one replicate of the 30 N treatment.

Discussion

According to our expectations, species compositional shifts with increasing nutrient concentration towards the larger diatom were reflected in changes in mean community cell size,

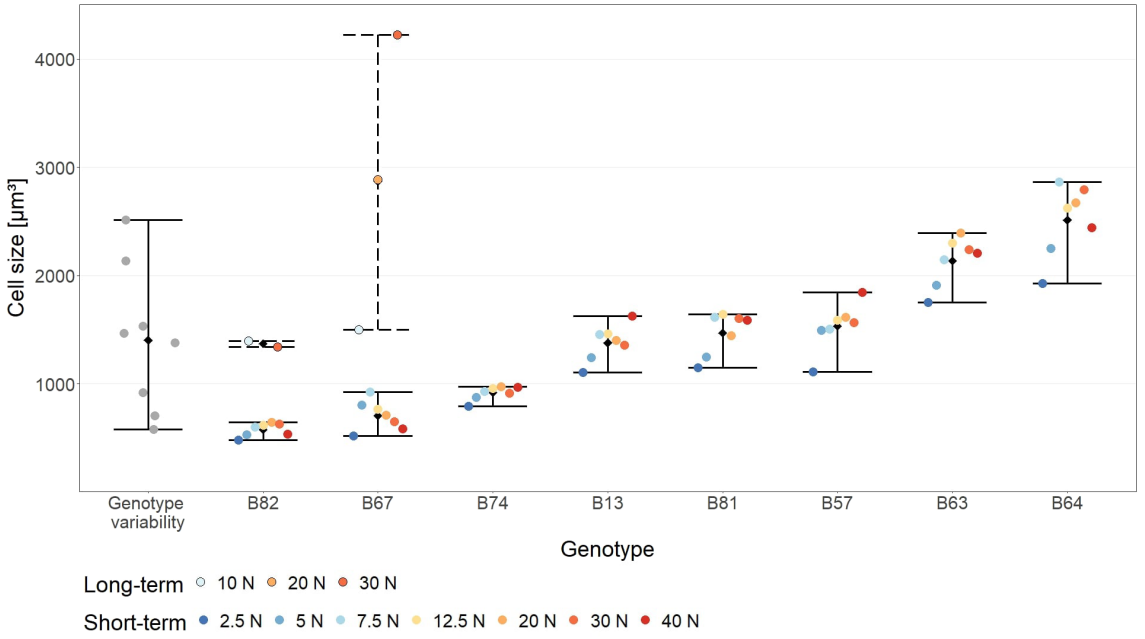

Figure 5. Short-term reaction norms of cell size for each *C. affinis* genotype are shown as the solid line ranges of mean size values measured in the different nutrient levels (coloured dots). Among genotype variability (left side) in the short-term plasticity experiment is shown as the solid line range of mean cell sizes of each genotype averaged across nutrient level. Observed phenotypic variability of genotypes B82 and B67 that remained in more than one replicate to the end (175 days) of the long-term community experiment is visualised by the dashed line ranges of average size values in the different nutrient regimes. The coloured dots associated to the dashed lines showing the mean cell size in each of the three applied nutrient regimes in the long-term community experiment.

total abundance and biomass. Intraspecifically, the observed increase in size and biomass and decline in abundance towards higher nutrient concentrations, contrary to our expectation, could not be connected to directional genotype sorting according to their initially measured mean cell size. Instead, vast size variability of one remaining *C. affinis* genotype emerged towards the end of the community experiment and explained the observed species' size response to nutrients. In fact, this genotype's emerged size variability reflected the trait flexibility that allowed for morphotype sorting in response to nutrient regimes and ultimately explained intraspecific shifts in cell size. These intraspecific shifts with time not only added and thus translated to the observed increase in mean community size with nutrients, but also contributed to a rise in total biomass in replete nutrient conditions (reflected in the interaction between nutrients and time in Table 2 and the Supporting information). The fact that the size variability of one remaining *C. affinis* genotype at the end of the community experiment exceeded the genotype's short-term reaction norm in cell size towards nutrients excludes the possibility for selection of genotypes exhibiting substantial short-term plasticity. Instead, the data suggest selection for a highly plastic genotype only in the longer term, which was likely possible through increased intragenotypic variability by the formation of asexual auxospore-resembling cells.

Responses and consequences of species compositional shifts

The responses of mean community cell size, total abundance and biomass to nutrient regimes met our expectations and can be related to the observed species' compositional shifts and their resource use. The dominance of the larger *C. affinis* under the highest nutrient concentration was as projected since diatoms are known to rapidly grow (Maranon 2015) and as velocity-adapted species outcompete smaller species in pulsed and nutrient-replete conditions (Sommer 1984, Litchman 2007). The nitrate concentrations in the 10 and 20 N regimes apparently were low enough to allow the affinity-adapted *E. huxleyi* to thrive and successfully compete which resulted in an even biomass composition of the two species. While mean community cell size increase and subsequent total abundance decline was most pronounced between the 20 and 30 N treatments and can be explained by the nutrient-driven increase in dominance of the larger *C. affinis*, the major increase in total biomass occurred from the 10 to 20 N nutrient regimes. Here, the even distribution of both species remained constant because both species gained from the increased resource availability. This likely led to complementary resource use between the two species and translated to the significant increase in total biomass with nutrients. Two possible and likely non-exclusive interpretations can explain the lesser increase in total biomass from the 20 to 30 N treatment. First, non-complementary nutrient use due to the dominance of *C. affinis*. Second, P-limitation according to the manipulated N:P ratio has led to unused nitrate (Supporting information).

Intraspecific dynamics: genotype sorting, possible plasticity, morphotype distribution

We did not observe selection on standing genotypic variation in cell size in the different nutrient treatments, which we expected to happen in particular for genotypes of *C. affinis* due to their pronounced variation in mean cell size before the onset of the community experiment (Supporting information). Instead, the most probable explanation is that genotype selection took place for the most plastic genotype (B67) in the long-term. For this genotype (B67), in parallel to genotype competitive exclusion, the emerged size variability was reflected in the occurrence of differentially sized morphotypes at the end of the community experiment. The different morphotypes in turn allowed for size-related sorting towards nutrients which likely reflected the genotype's plasticity. According to our expectations, the highest nitrate concentration mainly selected for the large morphotype, whereas also smaller-sized morphotypes contributed to the genotype's biomass at lower nitrate concentrations (Fig 4). At the same time the observed size variability of this one genotype translated to an increase in variability of all *C. affinis* size-related variables (Supporting information). The size selection again can be explained by the fact that smaller cells due to higher surface-to-volume ratio are better adapted to use, and thus compete for, the available resources in low nutrient concentrations (Aksnes and Egge 1991, Sommer et al. 2016). In contrast, while showing lower affinity, larger cells are often better suited to rapidly take up pulses of highly concentrated nutrients as simulated in the 30 N nutrient regime (Sommer 1984). Different morphotypes also occurred for genotype B82. Here, only medium-sized cells were present in the highest nutrient regime while large and small cells coexisted in the lowest. This distribution, however, did not lead to differences in mean size among the two nutrient treatments (only one and two replicates were available for the 30 N and 10 N nutrient treatments, respectively) in which this genotype remained as monodominant. For the third genotype (B13) we could not evaluate for size variability as it only monodominated one single replicate in the 30 N regime.

In our study genotyping involved some constraints due to limited data. For the analysis of genotype sorting over time, we excluded replicates in which less than five cells could be genotyped for a species. To the extreme, this led to the exclusion of seven out of 15 replicates across nutrient regimes for *C. affinis* at the end of the community experiment. The analysis of size variability of the two less abundant *C. affinis* genotypes (B82, B13) at the end of the experiment was largely limited as they monodominated very few replicates.

The evolution of cell size variability and the specific role of the diatom life cycle for plasticity

The observed phenotypic variability in cell size of one *C. affinis* genotype (B67) that monodominated replicates in all nutrient regimes at the end of the long-term community experiment clearly exceeded the measured reaction norms

of the corresponding but also of all other genotypes in the short-term plasticity experiment. From this, we exclude the possibility that the observed size variability originated from evolution through selection of genotypes being highly plastic from the beginning. We exclude evolution of size plasticity caused by sexual recombination as the applied microsatellite markers were able to identify the original nine *C. affinis* genotypes throughout the entire experiment. We further assume adaptive evolution due to undirected mutations over the 130 generations covered in our experiment is unlikely to explain our results of significant size variability. For example, Lohbeck et al. (2012) found changes in growth rate and cell size caused by mutations of the faster-growing species *Emiliania huxleyi* in our system after 500 generations. They calculated that after the occurrence of mutations, the sweep time to increase mean population fitness by 2.5 to 5% alone took about 110 to 205 generations. In our community experiment, such a sweep period basically would have left no time for mutations to play an ecological role. They are therefore unlikely to explain the observed doubling in intraspecific size from the point intra-genotypic variability emerged. Others likewise show that nutrient-dependent thermal adaptation of diatoms did not occur before 200 generations (Aranguren-Gassis et al. 2019). Therefore, we consider the most probable explanation for our findings to be evolution of size plasticity through selection of the most plastic genotype (B67) in the long term. Unfortunately, we cannot ultimately prove evolution of plasticity as we did not conduct a second plasticity experiment with the three remaining genotypes since we were not aware of these findings at the termination of the community experiment. Our data suggest, however, that the possible evolution of size plasticity towards nutrient availability in the community experiment did not occur before 120 days because from this point cell size and variability of all *C. affinis* size-related responses started to increase in all nutrient treatments (Fig. 2, Supporting information). We assume, that from this point on the most plastic genotype (B67) showed long-term life cycle-related cell size shifts pointing to possible developmental plasticity of cell size. A closer look revealed that the observed *C. affinis* cell size increase was driven by the increase in radius, i.e. the increasing diameter, of the cylindric cells (Supporting information). In contrast to the height, the radius affects the volume of a cylinder in a quadratic manner (volume cylinder = pi r^2 h, where r describes the radius and h the height of the cylinder). Thus, small changes can cause significant size shifts. Particularly, at the end of the community experiment in the 30 N nutrient regime, the radius increased by approximately 3 µm over 28 days and led to the unexpectedly strong increase in diatom size (Supporting information). However, according to common literature, diatoms cannot increase their diameter through clonal cell reproduction, during which normally each half of a divided cell turns into an epitheca and generates a new naturally smaller hypotheca, respectively. This process leads to a gradual decline of cell size in clonal populations until auxosporulation takes place, which usually involves sexual reproduction. Auxosporulation results in the formation of a larger initial cell of original size from which the vegetative cycle starts from the beginning (Kaczmarska et al. 2013). Therefore, it should not be possible for a clonal diatom cell to show a purely physiological response in size via increasing the diameter. However, Kaczmarska et al. (2013) also reported the exception from the rule, namely the formation of an auxospore-resembling cell without sexual recombination allowing for cell size recovery of a clonal population by increasing the diameter after becoming gradually small. In our long-term experiment, the gradual decline in diameter and hence cell size until 125 to 160 days depending on the nutrient regime (Supporting information) points to clonal reproduction via cell divisions. This phase was followed by a pronounced increase in diameter (Supporting information), which suggests cell size recovery through vegetative formation of an auxospore-resembling cell. A similar pronounced increase (doubling) in cell size of a different centric diatom species due to the suggested asexual formation of auxospore-resembling cells has been reported (Godhe et al. 2014). Godhe and Rynearson (2017) pointed out that diatom life cycle traits such as the formation of resting and auxospores can potentially affect the phenotypic variability of a particular population which would be confirmed by our finding. However, we have not actively monitored the samples for auxospore-resembling cells and thus can neither ultimately confirm nor exclude the occurrence of the proposed asexual cell size recovery. Independent of the exact mechanism that has led to the possibly emerged high plasticity, we suggest that intragenotypic variability, which was likely provided by asexual auxosporulation, enabled selection of cells with a wider diameter. This allowed for the resulting morphotype distribution with on average significantly larger cells under higher nutrient availability at the end of the long-term community experiment.

The potential causes and consequences of plasticity in a community context

Understanding intraspecific trait variability and in particular the causes and consequences of plasticity in of the light of community diversity is a fascinating and highly integrative area of ecology which so far remains rarely addressed. The suggested evolved size plasticity through selection of *C. affinis* genotype B67 covered a cell size range that was similar to both the interspecific cell size variation between *C. affinis* and *E. huxleyi* at the onset of the community experiment (Supporting information) and the intraspecific variation measured among all *C. affinis* genotypes during the plasticity experiment (Fig. 5). In other words, the possibly evolved plasticity covered trait variability of a similar magnitude at the end of the community experiment as across species and genotypes at the onset. In communities, interspecific diversity can act as a self-stabilizing force, constraining intraspecific variability by limiting a species' niche occupancy (Ellers 2009). Our results can be used to extend this idea to the interaction between genotype diversity and plasticity, suggesting that a decrease in genotype diversity could weaken the stabilizing effect, potentially resulting in significant plastic responses

in cell size of a single genotype across various nutrient treatments. While we cannot say whether the suggested evolution of plasticity in our experiment was only possible because of low genotype richness, or whether it was possible due to ecologically uncorrelated diatom auxospore formation, the data suggest that rapid evolution of plasticity could be a mechanism to maintain trait diversity during bottleneck situations of low species and/or genotype richness.

The major consequence of the possibly emerged plasticity in our study was that the resulting intraspecific cell size increase of *C. affinis* not only added to the increase in mean community cell size but also to a rise in total biomass in replete nutrient conditions. In other words, plastic trait changes of one genotype translated to the functional community level. There are only very few examples in the literature on the functional community ecological role of phenotypic plasticity. For example, Lajoie and Vellend (2018) suggested that community-level trait responses in herbaceous plants to ongoing climate change were predominantly mediated by species turnover, similar to our findings. Those trait changes that could be attributed to intraspecific dynamics, however, were mainly driven by plasticity and not genetic differentiation among populations, i.e. evolutionary change. In a field experiment testing the effects of diversity on productivity through crown light use of young trees, Williams et al. (2017) demonstrated that neighbourhood-driven plasticity in crown morphology contributed equally to complementarity-driven overyielding than interspecific differences. These few studies including our findings presented here, however, do not allow to generalise the importance of plasticity driving community-level trait changes. The role of trait plasticity is likely context-dependent and might come into play when other sources of trait variability in a community are rare as we have discussed above. For phytoplankton, such an integrated demonstration of the importance of different trait change drivers has not been conducted so far. However, Malerba et al. (2016) underpin that considering mean trait values of phytoplankton species only, while disregarding plastic intraspecific variability, can lead to an underestimation of the physiological performance of a species by an order of magnitude. The authors showed that in chlorophyte phytoplankton intraspecific cell size plasticity significantly affected nutrient utilization-related traits, which are known to be important for phytoplankton competitive success and thus community structure and functioning (Litchman et al. 2007). In line with our findings, these insights call for the recognition of plasticity as a source of trait variability when predicting future phytoplankton changes using mathematical models as stated in Acevedo-Trejos et al. (2022). In particular, the plasticity of size is important, because it was shown that phytoplankton diversity is largely regulated via two size-mediated tradeoffs, i.e. the competition-vulnerability and the affinity-growth tradeoff (Vallina et al. 2014).

While the overall finding that replete nutrient concentrations select for larger cells is not new, the novelty of our study is that we not only demonstrate the occurrence of selection on the species, genotype and plastic level in a community context but also their ecological relevance. The generality of our finding might be limited by studying a community with two species and 18 genotypes only. Applying such a simplified system, however, demonstrates the classic tradeoff between a controlled model community to understand each of the ongoing processes and natural ecosystems which exhibit many more simultaneously occurring dynamics and thus variability. A next step of major interest in the future that could build upon this study is to experimentally quantify the contributions to community-level changes not only of inter- and intraspecific trait changes (Hattich et al. 2022) but intraspecifically to partition also those of genotype sorting and plasticity. For this purpose, one could apply the partitioning approach after Stoks et al. (2016), which requires isolation, cultivation and reaction norm measurements of potentially evolved genotypes. Another potential way to tackle this complex task could be flexible model-based hypothesis testing (Pantel and Becks 2023) which can compare and predict the outcome among alternative eco-evo-physiological hypotheses including their interactions. Such an approach would require new data acquirements, particularly the measure of original and potentially evolved plasticity.

Conclusions

In this study, we show that implying all three levels on which trait diversity in a community can be exhibited are potentially important to explain community-level trait and functional changes. In an experimental phytoplankton model community, changes in mean cell size and total biomass in response to different nutrient regimes could likely be explained by the expected composition of the two species. Genotype sorting according to their mean cell size did not add to the explanation in the first place. Intraspecifically, however, possible evolution of size plasticity of one of the genotypes allowed for size-related selection and distribution of morphotypes, which ultimately provided the intraspecific response diversity in the different nutrient regimes. Importantly, the fact that size variability in this community was of similar magnitude, no matter if exhibited through species and genotype variability or phenotypic plasticity, allowed the possibly evolved plasticity in cell size to translate to community-level trait and functional shifts. Our results demonstrate that predicting the fate of (phytoplankton) communities heavily relies on considering the multiple and interchangeable ways by which communities can maintain trait variability and hence respond to changing environmental conditions.

Acknowledgements – We kindly acknowledge the various help and advice in the lab by J. Romberg, S. M. Marten, K. Qelai, H. Rickels, D. Gill, J. Houvener, S. Antoniello, J. Eberle, T. Liese, J. Throm, K. Seebass, L. Hansen, J. Hoffmann, A. Fabricius and V. Frey. We thank Ulf Riebesell and Arne Körtzinger for providing lab space and technical support, and Sabine Flöder for friendly review of an earlier version of this manuscript.

Funding – Main funding was provided through DFG priority program SPP 1704 DynaTrait: Grant to Birte Matthiessen MA5058/2-2 and grant to Thorsten Reusch RE1708/17-2. The research stay of Silvia Pulina was funded by the German Academic Exchange Service (DAAD) and the Programma Mobilità Giovani Ricercatori of the University of Sassari (Italy).

Author contributions

Birte Matthiessen: Conceptualization (lead); Formal analysis (equal); Funding acquisition (lead); Investigation (equal); Methodology (equal); Project administration (lead); Resources (equal); Supervision (lead); Validation (equal); Writing - original draft (lead); Writing - review and editing (equal). **Giannina S. I. Hattich:** Conceptualization (equal); Investigation (equal); Methodology (equal); Writing - review and editing (equal). **Silvia Pulina:** Funding acquisition (supporting); Investigation (equal); Methodology (equal); Writing - review and editing (equal). **Thomas B. H. Hansen:** Investigation (equal); Methodology (equal); Validation (equal); Writing - review and editing (equal). **Thorsten B. H. Reusch:** Funding acquisition (supporting); Methodology (equal); Resources (equal); Writing - review and editing (equal). **Jorin Hamer**: Data curation (lead); Formal analysis (lead); Investigation (equal); Methodology (equal); Validation (equal); Visualization (lead); Writing - original draft (equal); Writing - review and editing (equal)

Data availability statement

Data are available from the Pangaea Repository: https://doi.pangaea.de/10.1594/PANGAEA.957930 (Matthiessen et al. 2024).

Supporting information

The Supporting information associated with this article is available with the online version.

References

Acevedo-Trejos, E., Cadier, M., Chakraborty, S., Chen, B., Cheung, S. Y., Grigoratou, M., Guill, C., Hassenrück, C., Kerimoglu, O., Klauschies, T., Lindemann, C., Palacz, A., Ryabov, A., Scotti, M., Smith, S. L., Våge, S. and Prowe, F. 2022. Modelling approaches for capturing plankton diversity (MODIV), their societal applications and data needs. – Front. Mar. Sci. 9: 975414.

Acevedo-Trejos, E., Maranon, E. and Merico, A. 2018. Phytoplankton size diversity and ecosystem function relationships across oceanic regions. – Proc. R. Soc. B 285: 20180621.

Aksnes, D. L. and Egge, J. K. 1991. A theoretical model for nutrient uptake in phytoplankton. – Mar. Ecol. Prog. Ser. 70: 65–72.

Aranguren-Gassis, M., Kremer, C. T., Klausmeier, C. A. and Litchman, E. 2019. Nitrogen limitation inhibits marine diatom adaptation to high temperatures. – Ecol. Lett. 22: 1860–1869.

Bates, D., Mächler, M., Bolker, B. and Walker, S. 2015. Fitting linear mixed-effects models using lme4. – J. Stat. Softw. 67: 1–48.

Cardinale, B. J., Wright, J. P., Cadotte, M. W., Carroll, I. T., Hector, A., Srivastava, D. S., Loreau, M. and Weis, J. J. 2007. Impacts of plant diversity on biomass production increase through time because of species complementarity. – Proc. Natl Acad. Sci. USA 104: 18123–18128.

Cardinale, B. J., Bennett, D. M., Nelson, C. E. and Gross, K. 2009. Does productivity drive diversity or vice versa? A test of the multivariate productivity–diversity hypothesis in streams. – Ecology 90: 1227–1241.

Cardinale, B. J., Duffy, J. E., Gonzalez, A., Hooper, D. U., Perrings, C., Venail, P., Narwani, A., Mace, G. M., Tilman, D., Wardle, D. A., Kinzig, A. P., Daily, G. C., Loreau, M., Grace, J. B., Larigauderie, A., Srivastava, D. S. and Naeem, S. 2012. Biodiversity loss and its impact on humanity. – Nature 486: 59–67.

Des Roches, S., Post, D. M., Turley, N. E., Bailey, J. K., Hendry, A. P., Kinnison, M. T., Schweitzer, J. A. and Palkovacs, E. P. 2018. The ecological importance of intraspecific variation. – Nat. Ecol. Evol. 2: 57–64.

Edwards, K. F., Thomas, M. K., Klausmeier, C. A. and Litchman, E. 2012. Allometric scaling and taxonomic variation in nutrient utilization traits and maximum growth rate of phytoplankton. – Limnol. Oceanogr. 57: 554–566.

Ellers, J. 2009. Evolutionary processes in community ecology. – In: Verhoef, H. A. and Morin, P. J. (eds), Community ecology: process, models and applications. Oxford Univ. Press, pp. 151–162.

Finkel, Z. V., Beardall, J., Flynn, K. J., Quigg, A., Rees, T. A. V. and Raven, J. A. 2010. Phytoplankton in a changing world: cell size and elemental stoichiometry. – J. Plankton Res. 32: 119–137.

Fussmann, G. F., Loreau, M. and Abrams, P. A. 2007. Eco-evolutionary dynamics of communities and ecosystems. – Funct. Ecol. 21: 465–477.

Godhe, A. and Rynearson, T. 2017. The role of intraspecific variation in the ecological and evolutionary success of diatoms in changing environments. – Phil. Trans. R. Soc. B 372: 20160399.

Godhe, A., Kremp, A. and Montresor, M. 2014. Genetic and microscopic evidence for sexual reproduction in the centric diatom *Skeletonema marinoi*. – Protist 165: 401–416.

Govaert, L., Pantel, J. H. and De Meester, L. 2016. Eco-evolutionary partitioning metrics: assessing the importance of ecological and evolutionary contributions to population and community change. – Ecol. Lett. 19: 839–853.

Gross, K. and Cardinale, B. J. 2007. Does species richness drive community production or vice versa? Reconciling historical and contemporary paradigms in competitive communities. – Am. Nat. 170: 207–220.

Guillard, R. R. L. 1975. Culture of phytoplankton for feeding marine invertebrates. – Cult. Mar. Invertebr. Anim. 29–60.

Hairston Jr, N. G., Ellner, S. P., Geber, M. A., Yoshida, T. and Fox, J. A. 2005. Rapid evolution and the convergence of ecological and evolutionary time. – Ecol. Lett. 8: 1114–1127.

Hamer, J., Matthiessen, B., Pulina, S. and Hattich, G. S. I. 2022. Maintenance of intraspecific diversity in response to species competition and nutrient fluctuations. – Microorganisms 10: 113.

Hattich, G. S. I., Listmann, L., Raab, J., Ozod-Seradj, D., Reusch, T. B. H. and Matthiessen, B. 2017. Inter- and intraspecific phenotypic plasticity of three phytoplankton species in response to ocean acidification. – Biol. Lett. 13: 20160774.

Hattich, G. S. I., Listmann, L., Govaert, L., Pansch, C., Reusch, T. B. H. and Matthiessen, B. 2022. Experimentally decomposing phytoplankton community change into ecological and evolutionary contributions. – Funct. Ecol. 36: 120–132.

Hattich, G. S. I., Listmann, L., Havenhand, J., Reusch, T. B. H. and Matthiessen, B. 2023. Temporal variation in ecological and evolutionary contributions to phytoplankton functional shifts. – Limnol. Oceanogr. 68: 297–306.
Hein, M., Pedersen, M. F. and Sand-Jensen, K. 1995. Size dependent nitrogen uptake in micro- and macroalgae. – Mar. Ecol. Prog. Ser. 118: 247–253.
Hillebrand, H., Dürselen, C.-D., Kirschtel, D., Pollingher, U. and Zohary, T. 1999. Biovolume calculations for pelagic and benthic microalgae. – J. Phycol. 35: 403–424.
Hillebrand, H., Acevedo-Trejos, E., Moorthi, S. D., Ryabov, A., Striebel, M., Thomas, P. K. and Schneider, M.-L. 2022. Cell size as driver and sentinel of phytoplankton community structure and functioning. – Funct. Ecol. 36: 276–293.
Hutchinson, G. E. 1961. The paradox of the plankton. – Am. Nat. 95: 137–145.
Jacob, S. and Legrand, D. 2021. Phenotypic plasticity can reverse the relative extent of intra- and interspecific variability across a thermal gradient. – Proc. R. Soc. B 288: 20210428.
Kaczmarska, I., Poulíčková, A., Sato, S., Edlund, M. B., Idei, M., Watanabe, T. and Mann, D. G. 2013. Proposals for a terminology for diatom sexual reproduction, auxospores and resting stages. – Diatom Res. 28: 263–294.
Kester, D. R., Duedall, I. W., Connors, D. N. and Pytkowicz, R. M. 1967. Preparation of artificial seawater. – Limnol. Oceanogr. 12: 176–179.
Koch, H., Frickel, J., Valiadi, M. and Becks, L. 2014. Why rapid, adaptive evolution matters for community dynamics. – Front. Ecol. Evol. 2: 17.
Kuznetsova, A., Brockhoff, P. B. and Christensen, R. H. B. 2017. lmerTest package: tests in linear mixed effects models. – J. Stat. Softw. 82: 1–26.
Lajoie, G. and Vellend, M. 2018. Characterizing the contribution of plasticity and genetic differentiation to community-level trait responses to environmental change. – Ecol. Evol. 8: 3895–3907.
Lewandowska, A. M., Boyce, D. G., Hofmann, M., Matthiessen, B., Sommer, U. and Worm, B. 2014. Effects of sea surface warming on marine plankton. – Ecol. Lett. 17: 614–623.
Litchman, E. 2007. Resource competition and the ecological success of phytoplankton. – In: Falkowski, P. G. and Knoll, A. H. (eds), Evolution of primary producers in the sea. Elsevier, pp. 351–375.
Litchman, E. and Klausmeier, C. A. 2008. Trait-based community ecology of phytoplankton. – Annu. Rev. Ecol. Evol. Syst. 39: 615–639.
Litchman, E., Edwards, K. F., Klausmeier, C. A. and Thomas, M. K. 2012. Phytoplankton niches, traits and eco-evolutionary responses to global environmental change. – Mar. Ecol. Prog. Ser. 470: 235–248.
Litchman, E., de Tezanos Pinto, P., Edwards, K. F., Klausmeier, C. A., Kremer, C. T. and Thomas, M. K. 2015. Global biogeochemical impacts of phytoplankton: a trait-based perspective. – J. Ecol. 103: 1384–1396.
Litchman, E., Edwards, K. F. and Klausmeier, C. A. 2015. Microbial resource utilization traits and tradeoffs: implications for community structure, functioning, and biogeochemical impacts at present and in the future. – Front. Microbiol. 6: 254.
Litchman, E., Klausmeier, C. A., Schofield, O. M. and Falkowski, P. G. 2007. The role of functional traits and tradeoffs in structuring phytoplankton communities: scaling from cellular to ecosystem level. – Ecol. Lett. 10: 1170–1181.
Listmann, L., Hattich, G. S. I., Matthiessen, B. and Reusch, T. B. H. 2020. Eco-evolutionary interaction in competing phytoplankton: nutrient driven genotype sorting likely explains dominance shift and species responses to CO_2. – Front. Mar. Sci. 7: 634.
Lohbeck, K. T., Riebesell, U. and Reusch, T. B. H. 2012. Adaptive evolution of a key phytoplankton species to ocean acidification. – Nat. Geosci. 5: 917–917.
Malerba, M. E., Heimann, K. and Connolly, S. R. 2016. Nutrient utilization traits vary systematically with intraspecific cell size plasticity. – Funct. Ecol. 30: 1745–1755.
Maranon, E. 2015. Cell size as a key determinant of phytoplankton metabolism and community structure. – Annu. Rev. Mar. Sci. 7: 241–264.
Matthiessen, B., Hattich, G. S. I., Pulina, S., Hansen, T., Reusch, T. B. H. and Hamer, J. 2024. Data from: Phytoplankton mean cell size and total biomass increase with nutrients are driven by both species composition and evolution of plasticity. – Pangaea Repository, https://doi.pangaea.de/10.1594/PANGAEA.957930.
Pantel, J. H. and Becks, L. 2023. Statistical methods to identify mechanisms in studies of eco-evolutionary dynamics. – Trends Ecol. Evol. 38: 760–772.
Paul, C., Sommer, U. and Matthiessen, B. 2021. Composition and dominance of edible and inedible phytoplankton predict responses of Baltic Sea summer communities to elevated temperature and CO_2. – Microorganisms 9: 2294.
Peter, K. H. and Sommer, U. 2012. Phytoplankton cell size: intra- and interspecific effects of warming and grazing. – PLoS One 7: e49632.
Peter, K. H. and Sommer, U. 2013. Phytoplankton cell size reduction in response to warming mediated by nutrient limitation. – PLoS One 8: e71528.
Raffard, A., Santoul, F., Cucherousset, J. and Blanchet, S. 2019. The community and ecosystem consequences of intraspecific diversity: a meta-analysis. – Biol. Rev. 94: 648–661.
Schaum, E., Rost, B., Millar, A. J. and Collins, S. 2013. Variation in plastic responses of a globally distributed picoplankton species to ocean acidification. – Nat. Clim. Change 3: 298–302.
Siefert, A., et al. 2015. A global meta-analysis of the relative extent of intraspecific trait variation in plant communities. – Ecol. Lett. 18: 1406–1419.
Sommer, U. 1984. The paradox of the plankton: fluctuations of phosphorus availability maintain diversity of phytoplankton in flow-through cultures. – Limnol. Oceanogr. 29: 633–636.
Sommer, U. and Worm, B. 2002. Competition and coexistence. – Springer.
Sommer, U., Charalampous, E., Genitsaris, S. and Moustaka-Gouni, M. 2016. Benefits, costs and taxonomic distribution of marine phytoplankton body size. – J. Plankton Res. 39: 494–508.
Sommer, U., Stibor, H., Katechakis, A., Sommer, F. and Hansen, T. 2002. Pelagic food web configurations at different levels of nutrient richness and their implications for the ratio fish production:primary production. – Hydrobiologia 484: 11–20.
Stoks, R., Govaert, L., Pauwels, K., Jansen, B. and De Meester, L. 2016. Resurrecting complexity: the interplay of plasticity and rapid evolution in the multiple trait response to strong changes in predation pressure in the water flea *Daphnia magna*. – Ecol. Lett. 19: 180–190.
Valladares, F., Wright, S. J., Lasso, E., Kitajima, K. and Pearcy, R. W. 2000. Plastic phenotypic response to light of 16 congeneric shrubs from a Panamanian rainforest. – Ecology 81: 1925–1936.
Vallina, S. M., Follows, M. J., Dutkiewicz, S., Montoya, J. M., Cermeno, P. and Loreau, M. 2014. Global relationship between phytoplankton diversity and productivity in the ocean. – Nat. Commun. 5: 4299.

van Rij, J., Wieling, M., Baayen, R. and van Rijn, H. R. P. V. 2022. Itsadug: interpreting time series and autocorrelated data using GAMMs. – R package ver. 2.4.1.

Violle, C., Enquist, B. J., McGill, B. J., Jiang, L., Albert, C. H., Hulshof, C., Jung, V. and Messier, J. 2012. The return of the variance: intraspecific variability in community ecology. – Trends Ecol. Evol. 27: 244–252.

Williams, L. J., Paquette, A., Cavender-Bares, J., Messier, C. and Reich, P. B. 2017. Spatial complementarity in tree crowns explains overyielding in species mixtures. – Nat. Ecol. Evol. 1: 63.

Wood, S. N. 2011. Fast stable restricted maximum likelihood and marginal likelihood estimation of semiparametric generalized linear models. – J. R. Stat. Soc. 73: 3–36.